NEW ZEALAND SOCIETY FOR EARTHQUAKE ENGINEERING
2019 Pacific Conference on Earthquake Engineering
TURNING HAZARD AWARENESS INTO RISK MITIGATION
4 – 6 April | SkyCity, Auckland | New Zealand

Influence of flange detailing on the seismic performance of I-shaped reinforced concrete wall elements

J. Wang & K. Kusunoki
Earthquake Research Institute, The University of Tokyo, Japan

ABSTRACT

In Japan, monolithic reinforced concrete walls composed of in-plane and out-of-plane components, such as I-shaped walls, are often used in residential buildings. According to the “Standard for Structural Design of Reinforced Concrete Boxed-Shaped Wall Structures” by the Architectural Institute of Japan, the “flanges” of the I-shaped walls contribute to the resistance against seismic action acting parallel to the orientation of the “web”. Although there are recommendations to take this effect into consideration in design, the properties of the wall flange detailing, such as reinforcing configuration and flange geometry, are not explicitly considered. This study aims to address this demand by performing finite element analyses of an I-shaped reinforced concrete wall element. The analytical models are firstly calibrated against cyclic loading tests from an experimental study performed at Nagoya University. Various parameters of the flange component, such as the flange dimensions, reinforcing ratio, and reinforcement configuration, are varied to examine its effect on the wall’s seismic response. It is found that (i) increasing the flange length without modifying the reinforcing configuration, (ii) increasing the reinforcement within the flanges outside the effective region considered to contribute to the member’s capacity in design, and (iii) shifting the reinforcing bars within the flange further away from the section’s centroid consequently result in the increase in the strength of the wall element. Based on these results, recommendations considering the influence of flange detailing on the seismic performance of the I-shaped wall elements in design are proposed.

1 INTRODUCTION

Reinforced concrete wall structures, consisting of in-plane and out-of-plane walls and beam elements monolithically constructed together, are one of the most popular structure systems in Japan and has been widely used for residential apartment buildings. At times, the configuration of the in-plane and out-of-plane walls resembles an I-shape. There are often no column elements present, and all beam elements generally have the same width as the thickness of adjacent walls in this structural system.

Over the past few decades, it has been observed that this type of structural system has performed better than other types of reinforced concrete systems as detailed in reconnaissance reports from several previous earthquake events, such as Tohoku earthquake in 2011 (AIJ 2011), and Kumamoto earthquake in 2016 (AIJ 2018). Due to this, this type of structural system is deemed more favorable. To improve the performance of this structural system further, several studies, both experimental and analytical in nature, have since been conducted to investigate the seismic performance of wall structures.

One particular aspect that requires research is the consideration of an effective length within the flange walls. This is a region where the steel bars within the flange walls are assumed to contribute to the element's strength. In Japan, this length is assumed to be the smaller of six times the thickness of the adjacent bearing (i.e. web) wall or a quarter of the distance between the centroid of the flange walls (AIJ 2015). According to

$$ {}_{w}M_{u}=\Sigma\left(a_{t}\cdot\sigma_{y}\right)l'+0.5\Sigma\left(a_{w}\cdot\sigma_{wy}\right)l'+0.5N\cdot l' \tag{1}$$

$$ {}_{w}Q_{mu}={}_{w}M_{u}/h \tag{2}$$

$$ {}_{w}Q_{su}=\left(\frac{0.053p_{te}^{0.23}\left(F_{c}+18\right)}{M/\left(Q\cdot l\right)+0.12}+0.85\sqrt{p_{we}\cdot {}_{s}\sigma_{wy}}+0.1\sigma_{0e}\right)\cdot t_{e}\cdot j \tag{3}$$

the wall structure standard (AIJ 2015), the wall's flexural capacity in terms of bending moment, flexural capacity in terms of shear force, and the shear capacity can be calculated by Eqs. (1) to (3), respectively.

where, a_t: cross-sectional area of flexural reinforcement, σ_y: nominal yield strength of flexural reinforcement in one wall edge, l': equivalent length of bearing wall, taken as either (i) the length of the bearing wall if no out-of-plane walls are present or (ii) 0.9 times length of bearing wall if out-of-plane walls are present, a_w: cross-sectional area of flexural reinforcement in one wall intermediate portion, σ_{wy}: nominal yield strength of flexural reinforcement in one wall intermediate portion, N: Vertical force acting on bearing wall, p_{we}: vertical reinforcement ratio, p_{te}: tensile reinforcement ratio, F_c: concrete design strength, ${}_{s}\sigma_{wy}$: nominal yield strength of lateral reinforcement steel, σ_{0e}: the average normal stress of bearing wall, t_e: equivalent bearing wall thickness, j: distance between centres of stress (always calculated as 0.8 times l').

If seismic action acts in the direction of the I-shaped wall web, the reinforcing within the effective-length of the flange walls need to be considered in the cross-sectional area of flexural reinforcement, a_t, and the tensile reinforcement ratio, p_{te}, which plays a dominant role when calculating the moment and shearing force, as seen from Eqs. (1) to (3). However, as the effective length of the flange wall is solely based on the dimensions of the bearing wall, other properties of the flange, such as its dimensions, positioning of reinforcing bars, or amount of reinforcing provided outside of the effective region are not considered in calculating the flexural and shear strengths. In reality, these properties likely influence the performance of the structural wall. It has not been investigated whether the seismic performance of the wall may differ depending on the length of flange walls and the configuration of reinforcement within the flange walls.

This study aims to investigate the influence various parameters of the flange component on the strength of the whole I-shaped wall structure; in particular (i) the flange length, (ii) the amount of reinforcing bars within the flange outside the effective region considered to contribute to the member's strength in design, and (iii) location of reinforcing bars relative to the section's centroid location in the direction of applied seismic action . This is done using finite element analysis. The finite element model is firstly calibrated against results from an experimental study of I-shaped walls performed at Nagoya University (Teshigawara 2017), the description of which is provided in Section 2. The model's parameters of interest described previously are modified to evaluate its effect on the overall capacity of the wall.

2 DESCRIPTION ON WRC STRUCTURE EXPERIMENT

2.1 Specimen details

To calibrate the validity of finite element analysis modeling, the experimental and simulation results have been correlated and compared carefully and systematically.

As mentioned previously, the finite element model developed in this study is calibrated to experimental tests of I-shaped wall elements performed at Nagoya University (Teshigawara 2017). The wall specimens tested in their study are constructed at 1/2.5-scale. While several specimens are tested, this study only focuses on one specimen labeled 1NH. This specimen comprises a bearing wall and several flange walls as shown in Figure 1, and the dimensions and reinforcement details are summarized in Table 1. To better investigate the influence of flange on the bearing capacity, a slit is designed between the flange and loading slab to make sure that the loading (both of vertical and lateral loading) can transmit only to the bearing wall without affecting the flange. The properties of concrete and steel bars used in this specimen are summarized in Table 2 and Table 3, respectively.

Table 1: Design detail of specimens

Specimen		1NH
Bearing wall	width(mm) * height (mm)	80 * 1000
	longitudinal reinforcement	1-D6@100
	lateral reinforcement	1-D6@100
	end reinforcement	2-D10
Flange	width(mm) * height (mm)	80 * 710
	longitudinal reinforcement	1-D6@100
	lateral reinforcement	1-D6@100
	end reinforcement	2-D10

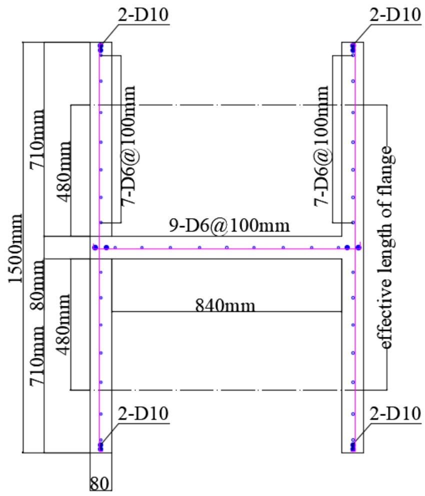

Figure 1: Specimen 1NH

Table 2: Properties of concrete

Specimen	Compressive strength (MPa)	Young Modulus ($\times 10^4$ MPa)	Tensile Strength (MPa)	Age (day)
1NH	27	2.52	2.19	46

Table 3: Properties of reinforcing steel

Steel No.	Yielding Strength (MPa)	Yielding Strain	Tensile Strength (MPa)	Modulus of Elasticity ($\times 10^4$ MPa)
D6	333	1850	492	1.82
D10	342	1795	495	1.91
D13	335	1783	490	1.88

2.2 Loading condition

The loading setup used in this experimental study is shown in Figure 2, where the constant vertical loads of total 135 kN are applied downward by two vertical actuators, and cyclic lateral loads are applied by the horizontal actuator. And the vertical load applied to the two hydraulic jacks includes the 135 kN to make sure that the inflection point can be just in the middle of the slab of the specimen. The entire cyclic loading process is controlled by the displacement of the slab.

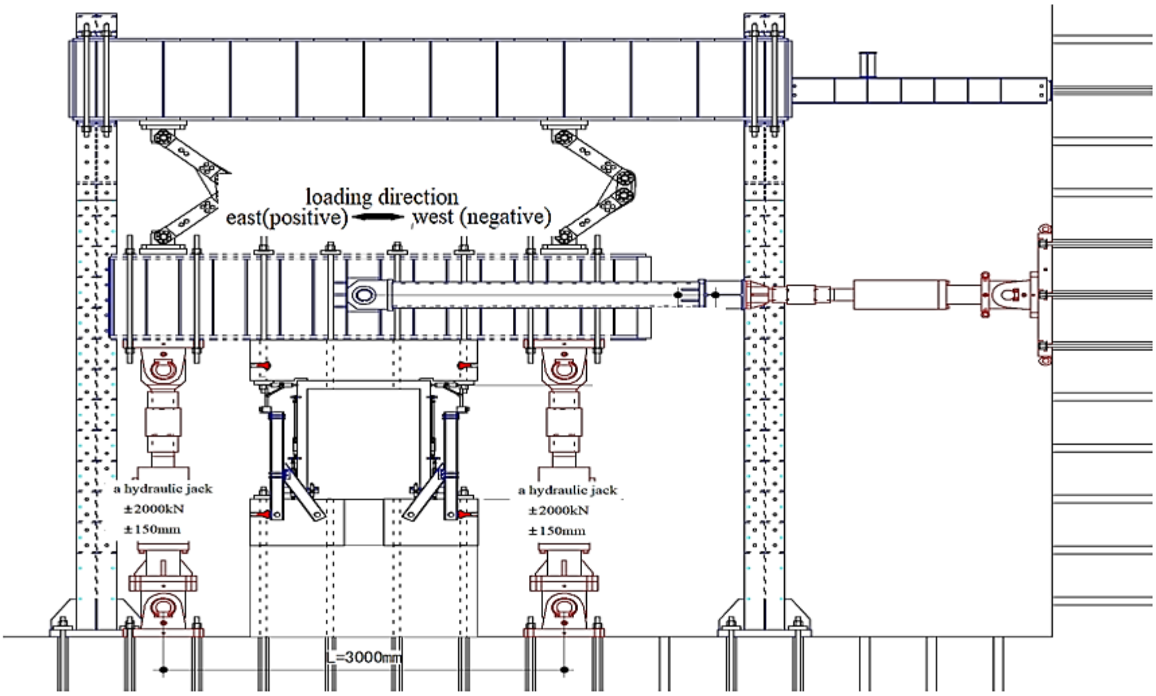

Figure 2: Loading equipment of testing at Nagoya University (Teshigawara 2017)

3 FINITE ELEMENT ANALYSIS

3.1 Model development

In this study, the configuration of the finite-element model is identical to the specimen tested at Nagoya University (Teshigawara 2017). The models of concrete and reinforcing steel bar used in the analysis are shown in Figure 3(a). The concrete is modeled using hexahedron elements consisting of 8 points for a single mesh and the reinforcing steel bar is modeled using truss element which is composed of 2 points.

The reinforced concrete material tensile stiffening model is adopted from Naganuma and Yamakuchi (1990), while the modified Ahmad model (Nakanuma 1995) is used for the ascending branch of the compressive stress-strain relationship and for the property of concrete compression softening. The cyclic stress-strain relationship of concrete under tensile and compression adopted in this study is that developed by Naganuma and Okubo (2000) which is shown in Figure 3(b).

Bilinear hysteresis behavior is assumed for the reinforcing steel. This is shown in Figure 3(c), where (i) the steel remains elastic till the yielding point is reached, (ii) strain hardening occurs with a stiffness of $0.01E_s$.

Finally, the bonding relationship between the common nodes of concrete and the reinforcing steel bar is modeled following Elmorsi (2000) and is shown in Figure 3(d).

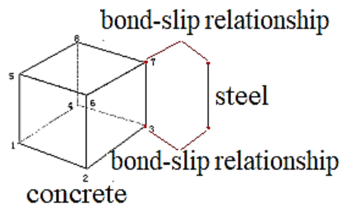

(a) Hexahedron element for concrete and truss element for steel bar

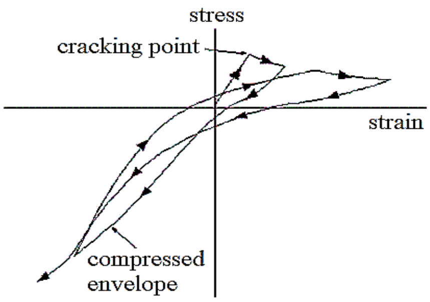

(b) Cyclic stress-strain relationship of concrete

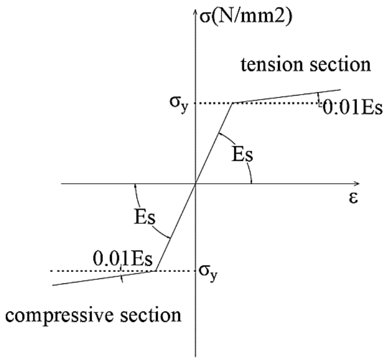

(c) Bilinear steel model
(Es:Young's modulus of steel)

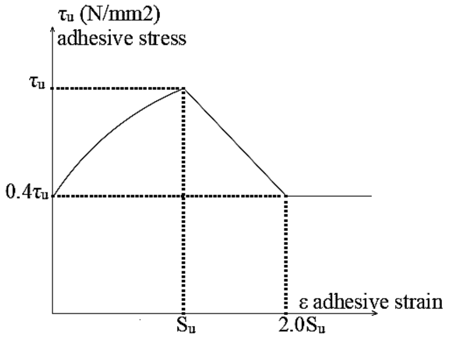

(d) Bond-slip deformations in reinforced concrete

Figure 3

3.2 Simulation and evaluation of calibrated model

The analyses are performed on a finite-element analytical software named FINAL (Obayashi Corporation 2018). The simulated model is shown in Figure 4. Figure 5 shows the comparison of the force-displacement curves between the experimental and simulation results. It is found that the model result matches the simulated result well, indicating that the modeling is acceptable and reliable for this type of structural system. Various properties of the model, such as the length of flanges, are thus modified. The effect of these modifications on the pushover response of the wall structures is discussed in Section 4.

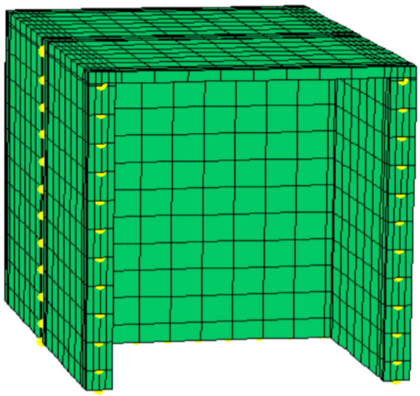

Figure 4: Illustration of model 1NH on FINAL

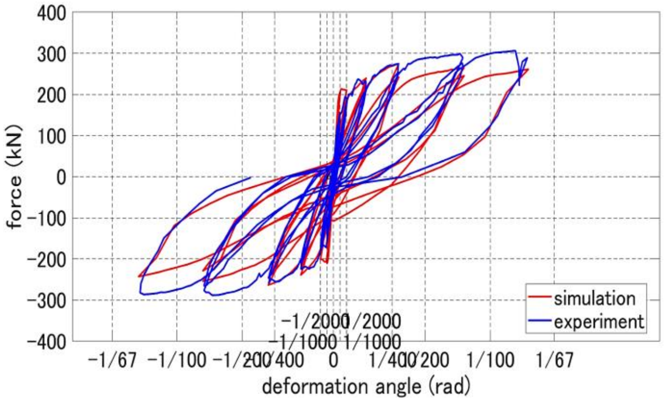

Figure 5: Comparison of finite-element model with experimental results

4 APPLICATION OF SIMULATION

This section examines the influence of flange wall properties on pushover response. In particular, three aspects of the wall properties are examined; (i) the length of the flanges, (ii) the reinforcing ratio in regions outside of the wall's effective length, and (iii) the location of reinforcing within the flanges (i.e. centroid of flange, closer towards outer edge, or closer towards web).

4.1 Length of flange

Based on Eq. (1), the length of flange is not considered in the calculation of the I-shaped wall's capacity. To investigate the validity of this exclusion, three models with different length of flange are adopted. The reinforcement configuration is kept identical in all three models while the length of flange has been set at 710 mm, 910 mm, and 1,110 mm as shown in Figure 6(a).

Figure 6(b) shows the comparison of strength of the three models. When the model experiences the deformation angle before 1/2000 rad, structures are in elastic phase and the force-displacement curves of these three models are almost the same. When the deformation angle increases, the lateral force of these three models begin to diverge, and it is obvious that the lateral force becomes larger as the length of flange increases longer till final stage. Overall, it is confirmed that the strength of the whole I-shaped wall structure is affected by length of flange and become larger as the length of flange increases.

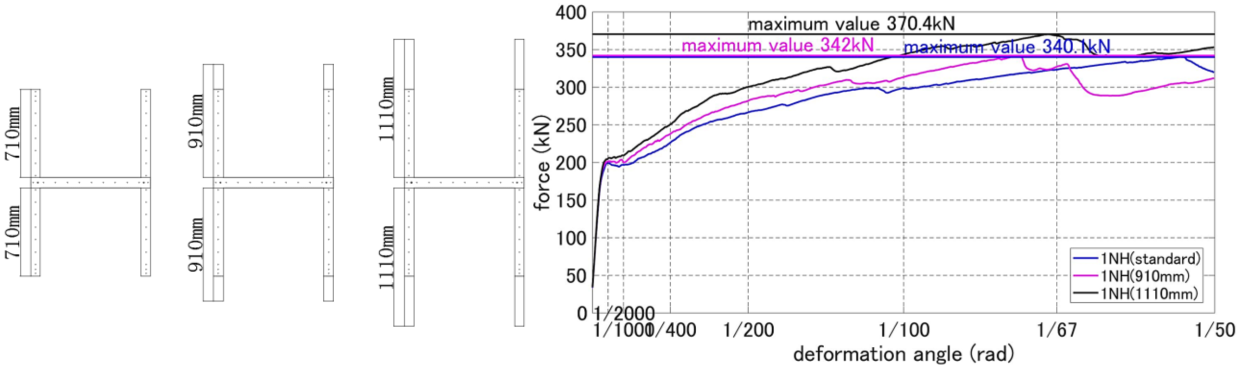

(a) Effect of modifying flange length *(b) Effect of modifying flange length*

Figure 6

4.2 Reinforcement in flange

The area of wall reinforcement in the flange region in Eq. (1) only considers the reinforcing present within the effective length of the flange walls. Thus, the whole flange has been divided into two parts; (i) the effective length zone, and (ii) outer zones. To investigate the effect of the reinforcing in the outer zone on the member's capacity, three models showed in Figure 7(a) are considered. Here, the reinforcing is varied between 2-D6+2-D10, 6-D6+2-D10, and 6-D6+6-D10 in the part of non-effective length of flange.

The comparison of three force-deformation curves is shown in Figure 7(b). When the structures experience the deformation angle before 1/2000 rad, the three models are in their elastic phase and the resulting force-displacement curves in this region are nearly identical. As the deformation angle increases, the value of lateral force is observed to diverge. Furthermore, it is can be found that the strength of models with less reinforcement (i.e. 2-D6+2-D10 and 4-D10) is smaller than the model with more steel bars. It is confirmed that the strength of the whole I-shaped wall structure is affected by the reinforcement in regions outside of the wall's effective length and become larger as the amount of reinforcement ratio increases.

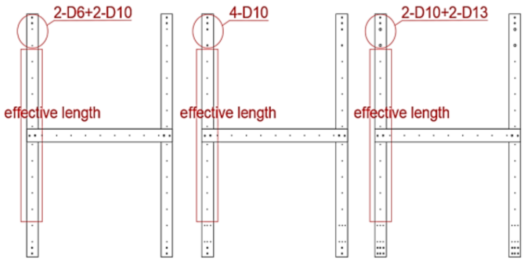

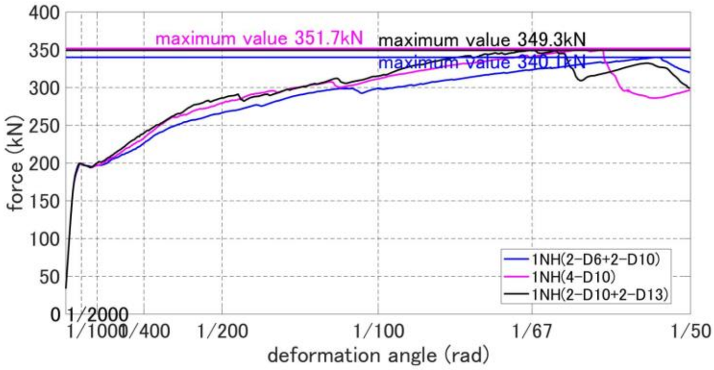

(a) Variation of reinforcing configuration outside of effective zone in flanges *(b) Effect of modifying reinforcing configuration*

Figure 7

4.3 Packing arrangement of reinforcement in flange

Another parameter not considered in Eq. (1) is the location of the steel reinforcing within the flange. For example, if the line of reinforcing within the flange is located further away from the web, the distance between the reinforcing and the section's neutral axis likely change, resulting in the section's capacity being modified. To investigate this, three models with different locations of the reinforcing steel bars in flanges shown in Figure 8(a) are considered.

Figure 8(b) shows the comparison of force-deformation curves of these three models. When the structure experiences a deformation angle before 1/2000 rad, the structures are kept in elastic phase and the force-displacement curves are almost the same. Up until the deformation angle of 1/100 rad, the force-displacement curve starts to display inelastic behavior, yet all three models are still nearly identical. Finally, when the deformation angle further increases, the three curves begin to diverge. It can be seen that the strength of models of 920mm and 960mm are still relatively similar. However, these are larger than that observed from the 880mm model.

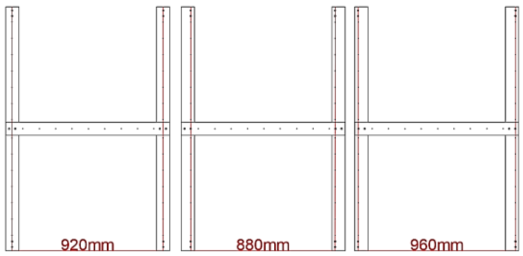

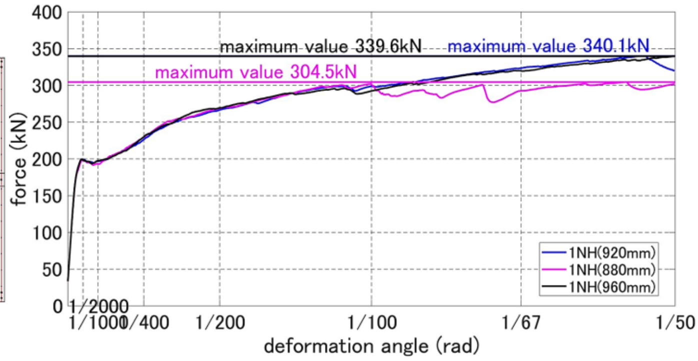

(a) Varying the location of reinforcing bars *(b) Effect of location of reinforcing bars*

Figure 8

5 CONCLUSIONS

Overall, it can be known from the simulation and experimental results described in this paper that:

(1) The FEM analysis is reliable for simulation of wall structure, and connected material models used in this study can be adopted for further research.

(2) The I-shaped wall capacity is influenced by:

i) The length of the flange walls, where an increase in wall length results in an increase in capacity.

ii) The amount of reinforcement outside of the effective-zones in the flanges, where an increase in outer-zones of flanges results in an increase in capacity.

iii) The reinforcement's location within the flange, where having the bars be located closer to the web resulted in a decrease in capacity, though this does not have a significant impact on the strength of the I-shaped structure.

6 FUTURE DIRECTION

Fundamental effects have been investigated for the strength of the I-shaped wall structure with regard to the length, reinforcement and packing arrangement of flange in this work, suggesting many new opportunities for future research on the topic of improving seismic performance of I-shaped reinforced concrete walls.

7 ACKNOWLEDGEMENT

The authors acknowledge the support of Teshigawara laboratory from Nagoya University for providing wall test data and a very helpful discussion.

8 REFERENCES

Architectural Institute of Japan. 2011. *Preliminary Reconnaissance Report of the 2011 Tohoku-Chiho Taiheiyo-Oki Earthquake*, Architectural Institute of Japan (AIJ)

Architectural Institute of Japan. 2015. *The standard for Structural Design of Reinforced Concrete Boxed-shaped Wall Structures*, Architectural Institute of Japan (AIJ)

Architectural Institute of Japan. 2018. Report on the Damage Investigation of the 2016 Kumamoto Earthquake, Architectural Institute of Japan (AIJ)

Elmorsi, M., Kianoush, M.R. & Tso, W.K. 2000. Modeling bond-slip deformations in reinforced concrete beam-column joints, *Canadian Journal of Civil Engineering*, Vol 27 490-505

Nakanuma, K. & Yamaguchi, T. 1990. Tension Stiffing Model under In-plane Shear Stress, *Summaries of technical papers of annual meeting of Architectural Institute of Japan*, Vol 1990 649-650

Nakanuma, K. 1995. Stress-strain Relationship for Concrete under Triaxial Compression, *Transactions of AIJ. Journal of structural and construction engineering*, Vol 60(474) 163-170

Nakanuma, K. & Ohkubo, M. 2000. An Analytical Model for Reinforced Concrete Panels under cyclic Stresses, *Transactions of AIJ. Journal of structural and construction engineering*, Vol 65(2000)536 135-142

Obayashi Corporation Technical Research Institute. 2018. *FINAL – 3D non-linear analysis for concrete structures*, Obayashi Corporation, Japan

Teshigawara, M., Takeuchi, K., Kamiya, T., Ohta, T., Kusunoki, K., Inai, E., Nakamura, A., Mukai, T. & Fukuyama, H. 2017. Study on Seismic Damage Control of WRC Structure (I: Outlines of test for the effect of orthogonal walls), *Summaries of technical papers of annual meeting of Architectural Institute of Japan*, Vol 2017 845-846